Evidence for Recent Groundwater Seepage and Surface Runoff on Mars

Michael C. Malin and Kenneth S. Edgett

Science **288**, 2330 (2000);
DOI: 10.1126/science.288.5475.2330

Science (print ISSN 0036-8075; online ISSN 1095-9203) is published weekly, except the last week in December, by the American Association for the Advancement of Science, 1200 New York Avenue NW, Washington, DC 20005.

Evidence for Recent Groundwater Seepage and Surface Runoff on Mars

Michael C. Malin* and Kenneth S. Edgett

Relatively young landforms on Mars, seen in high-resolution images acquired by the Mars Global Surveyor Mars Orbiter Camera since March 1999, suggest the presence of sources of liquid water at shallow depths beneath the martian surface. Found at middle and high martian latitudes (particularly in the southern hemisphere), gullies within the walls of a very small number of impact craters, south polar pits, and two of the larger martian valleys display geomorphic features that can be explained by processes associated with groundwater seepage and surface runoff. The relative youth of the landforms is indicated by the superposition of the gullies on otherwise geologically young surfaces and by the absence of superimposed landforms or cross-cutting features, including impact craters, small polygons, and eolian dunes. The limited size and geographic distribution of the features argue for constrained source reservoirs.

Present-day Mars is a desert world on which liquid water is not likely to be found at the surface, because average temperatures are below 273 K and atmospheric pressures are at or below water's triple-point vapor pressure of 6.1 mbar. However, in 1972 the Mariner 9 orbiter photographed evidence—in the form of giant flood channels and arborescent networks of small valleys—that liquid water (*1*) might have been stable in the surface environment at some time in the past (*2*–*8*). Analysis of Mars 4 and 5 (1974) and Viking orbiter images (1976–80) contributed to these views (*9*–*14*), as did observations of flood terrain by Mars Pathfinder in 1997 (*15*–*17*).

The Mars Global Surveyor (MGS) orbiter reached the planet in 1997 (*18*). One of the most important early results of the Mars Orbiter Camera (MOC) investigation was the absence of evidence for precipitation-fed overland flow. For example, there are no contributory rills, gullies, and/or small channels associated with the martian valley networks (*19*–*21*). MOC images instead suggest that most of the form and relief of the valley networks was created by collapse along paths dictated by slope and structure, but without obvious gradient continuity at the surface. It is possible—perhaps even likely—that surficial mantling and/or erosional processes have hidden or erased conduits and other surface manifestations of overland flow. Whatever the explanation for the absence of these features, the possibility that liquid water flowed across the martian surface in a sizeable volume for an extended period of time, and especially in the recent past, seems quite remote.

However, equally early in the MGS mission, MOC observations hinted at a more complex story regarding groundwater seepage. A few impact crater walls seen in images with spatial resolution of ~20 m/pixel displayed features resembling morphologies that, had they occurred on Earth, might be attributed to fluid seepage (*22*). Here we report on new high-resolution (2 to 8 m/pixel) images that more strongly indicate the occurrence of seepage-fed surface runoff.

Observations

Since the start of the mapping phase of the MGS mission (*18*), the MOC has acquired >20,000 images at scales of 1.5 to 12.0 m/pixel. The images cover from <1 km to a maximum of 3 km across, with lengths from a few to several hundred kilometers. With its body fixed to the spacecraft and without any independent means to point, the camera acquires nadir observations of selected features that pass below it (*23*).

As of January 2000, ~150 MOC images of ~120 locales (Fig. 1) show what we interpret as the results of fluid seepage and surface runoff. Three attributes of the observed landforms—the head alcove (representing a "source" morphology), the main and secondary channels (defining transportation conduits), and the depositional apron (Fig. 2)—are consistent with fluid-mobilized mass movement processes.

Geographic relations. Of the observed locales, about one-third are on interior walls or central peaks of impact craters, a quarter are on walls of distinctive pits in the south polar region, and a fifth are on walls of two major martian valley systems: Nirgal Vallis and Dao Vallis. Slightly less than 50% of all occurrences are found on south-facing slopes and ~20% face north. Features occur about two and a half times more often on poleward-facing slopes in a given hemisphere than they do on equator-facing slopes. More than 90% occur south of the equator, and with the exception of Nirgal Vallis (located at 27° to 30°S latitude), all are poleward of 30° latitude. Concentrations are found along the two valleys, in the polar pits, in craters and troughs associated with Gorgonum Chaos, and within the craters Hale, Maunder, Newton, and Rabe (Fig. 1).

Head alcove. The head alcove consists of the head- and sidewall escarpments, located below the brink of a slope, and the region of disrupted topography bounded by these scarps (Fig. 2). Alcoves are theater-shaped depressions within the wall or slope on which they have formed. Often, colluvium appears to have collected at the base of these escarpments, forming a wedge of debris climbing part of the way back up the head- and sidewall slopes. The bounding escarpments and

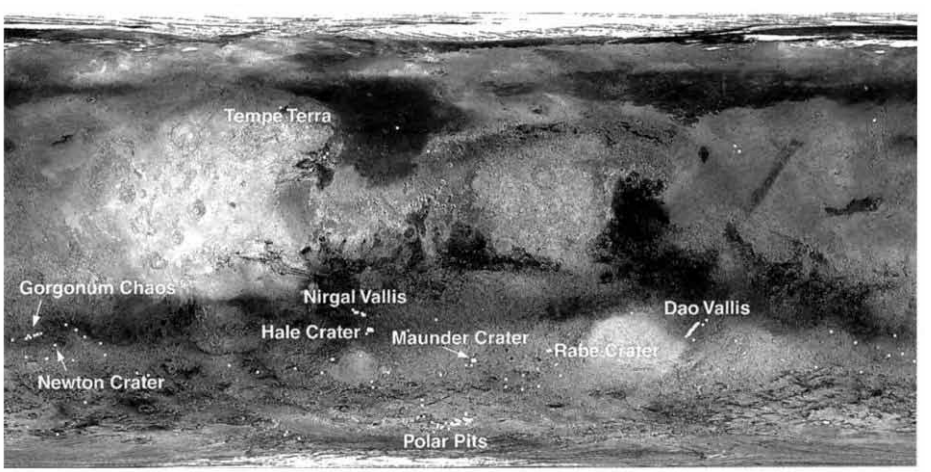

Fig. 1. Simple cylindrical equal angular map of Mars (centered on 0° latitude, 0° longitude) showing locations of gully landforms as found in images acquired through the end of January 2000.

Malin Space Science Systems, Post Office Box 910148, San Diego, CA 92191–0148, USA.

*To whom correspondence should be addressed.

mantling colluvium display rills with orientations that generally parallel slopes and gravity. Irregular mounds within the colluvium suggest that slumping and other, more surficial, mass movements contribute material from the slopes onto the floor of the alcove. In some areas, particularly south of 60°S, alcoves are commonly littered with large boulders (several meters to several decameters in diameter). The derivation of these boulders appears to be characteristic of the surface layer (or a near-surface layer) unique to this area. Rills in the colluvium contribute, across the floor of the alcove, toward the head of the main channel.

Four types of alcoves have been recognized: lengthened, widened, occupied, and abbreviated (Fig. 3). Lengthened alcoves are longer (downslope) than they are wide and commonly have subsidiary or contributing secondary alcoves or chutes (Fig. 3A). In the case of the polar pits, the abundance and distribution of elongated alcoves produce a "badlands" morphology (Fig. 3B). Widened alcoves are broad in transverse dimension (cross-slope) and can consist of more than one smaller alcove focusing to a single downslope outlet (Fig. 3C). Occupied alcoves are filled or partly filled with material that might be mobile as a unit, but not as disaggregated debris. The type examples of this form occur throughout the length of Dao Vallis (Fig. 3D). Abbreviated or attenuated alcoves are typical of areas of strong topographic or stratigraphic control of landform location. For example, in areas where a resistant rock unit creates an overhang, the alcove may be small or even missing (Fig. 3E). Other occurrences include some impact crater inner walls (Fig. 3F), where particularly steep topography may contribute to rapid downslope transport of material and upslope propagation of the landform.

The overall impression of the uppermost

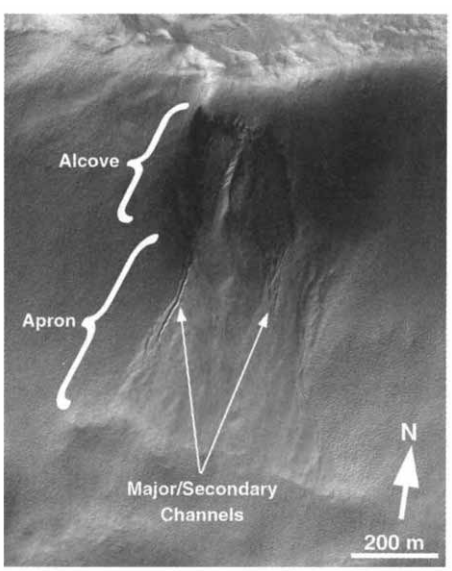

Fig. 2. Example of landforms that comprise the martian gullies. The three main geomorphic elements of these features are a theater-shaped alcove that tapers downslope, one or more major or secondary channels that continue downslope from the distal apex of the alcove, and triangular aprons that broaden downslope and appear to be material deposited after transport through the channel system. Illuminated from the upper left, this is a subframe of MOC image M03-00537, located near 54.8°S, 342.5°W.

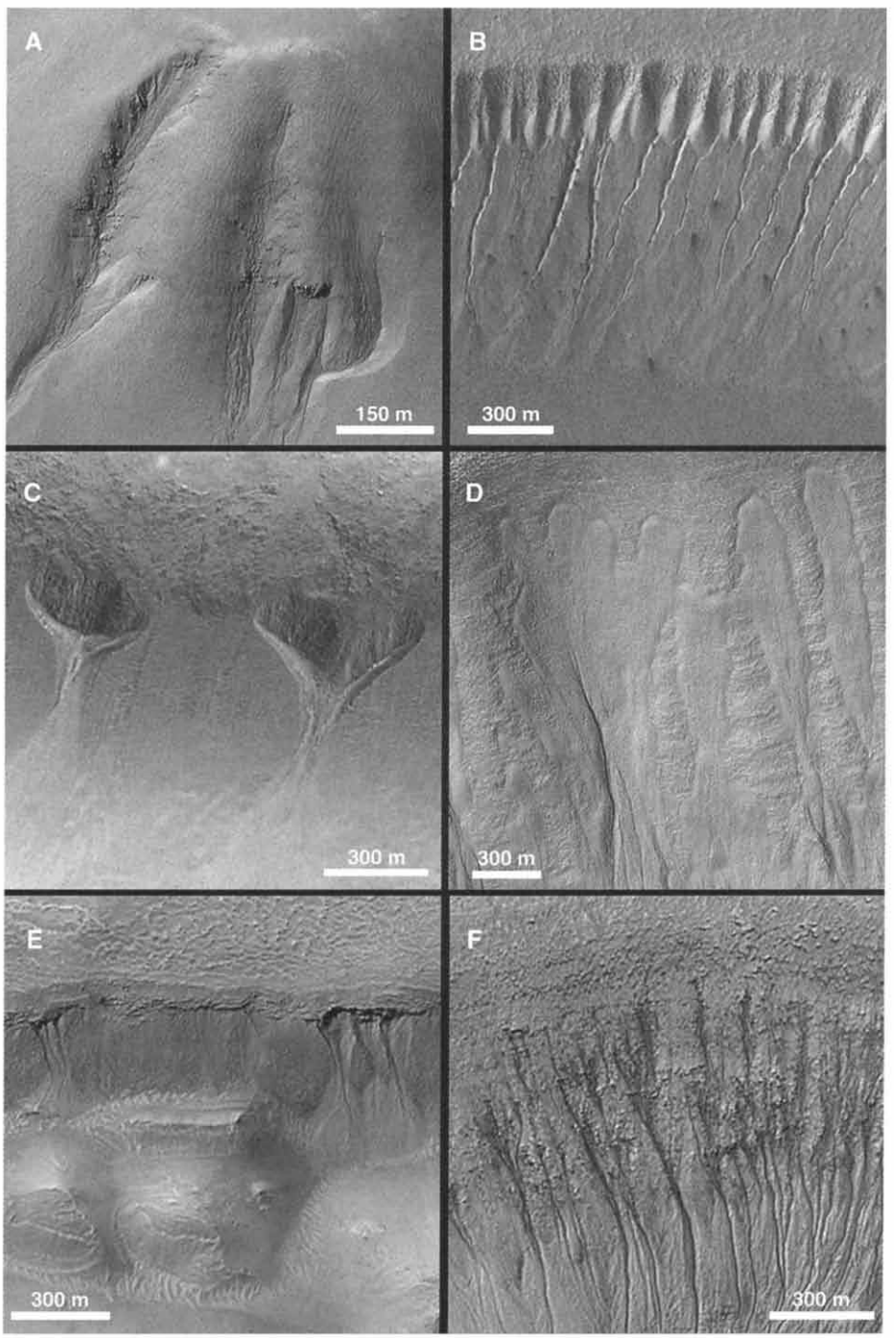

Fig. 3. Examples of alcoves. Lengthened alcoves (**A**) are longer (downslope) than they are wide; where they occur in close proximity, they form characteristic badlands (**B**). Widened alcoves (**C**) are broad in transverse dimension and may include more than one smaller alcove. Occupied alcoves (**D**) are those that appear to be filled with material. Abbreviated alcoves (**E** and **F**) show strong topographic or stratigraphic control of landform location, which limits the extent of the alcove. Each picture is a subframe of a MOC image illuminated from the upper left, except for (C), which is illuminated from the upper right, and (F), which is illuminated from the left: (A) image M07-05535 (54.8°S, 342.5°W); (B) image M03-02709 (70.8°S, 355.8°W); (C) image M03-02214 (58.9°S, 336.0°W); (D) image M11-01601 (33.1°S, 266.8°W); (E) image M07-02909 (38.5°S, 171.3°W); and (F) image M11-00944 (41.1°S, 159.8°W).

zone of these landforms is that a headland has experienced undermining and collapse across a confined zone, with downslope movement focused at or toward a point, and material moving under the force of gravity downslope toward an apex (the head of the main channel). These characteristics are shared by terrestrial seepage gullies and classic landslides (*24–29*).

Main and secondary channels. The most striking geomorphic aspect of these landforms is the occurrence of entrenched, steep-walled, V-shaped channels emanating from the downslope apex of the head alcove. In relation to other martian valleys and slope features, these channels are distinctive: They generally start broad and deep at their highest topographic position and taper downslope and distally (Figs. 4 and 5). Their courses are influenced by variations or undulations in surface relief and by subsurface processes; a small number are discontinuous (Fig. 6). Lineations adjacent to the main channel suggest secondary channels or alternative courses, now abandoned. The dominance of a single, deep, narrow path suggests that entrenchment mitigates channel migration. The transition between head alcove and channel can be abrupt or extended. In those areas where it is extended, there is in some places good evidence of the contributory nature of the process: "streamlining" behind obstacles, anastomosing patterns, and rapidly decreasing order (Fig. 7).

Depositional aprons. Surfaces downslope from the distal apex of the alcove display two distinct appearances. In the first of these forms, a crudely triangular zone or apron broadens downslope from the apex and continues to, and in some places beyond, the base of the slope hosting these features (Fig. 2). The surface of this zone may be smooth at the decameter scale, but it displays smaller swells and swales oriented downslope. These surfaces "host" the main and secondary channels, in the sense that the channels appear to cut down into the aprons. Many of the small swells are themselves wedge shaped, with their apices upslope. Swells often occur at the mouths of channels and are highest at the mouth of the channel and along a center line downslope from there, and their relief tapers marginally and distally. No lateral or distal terminal escarpments have been observed.

The second type of downslope pattern consists of distributary networks of small subsidiary channels (Fig. 5) and digitate flows (Fig. 8). Anastomosing channels, piracy, superposition, levees, distal and marginal escarpments, distal thickening, relief transitions from negative (channels) to positive (flows), and other attributes attest that the channels acted as conduits for the transport of material and that some may have been repeatedly occupied.

Age Relations

The proposed seepage landforms are not cratered: Only one apron in >150 examined has any craters at all visible in images with an average scale of 3 m/pixel. The absence of impact craters suggests that these landforms are geologically young (*30*). No examples of old, degraded seepage sites have been recognized. Rather, nearly all have other properties that also suggest relative youth, including superposition of aprons on eolian bedforms in Nirgal Vallis (Fig. 9A), superposition on polygonally patterned ground and the absence of rejuvenated polygons (Fig. 9B), and sharply defined topography and albedo patterns within the alcoves of some of the landforms

Fig. 4. Channels start broad and deep at their highest topographic position and taper downslope and distally. Many slopes show secondary channels or alternative courses, although one channel from each alcove clearly dominates. Illuminated from the upper left, this is a subframe of MOC image M07-01873, near 37.3°S, 168.0°W.

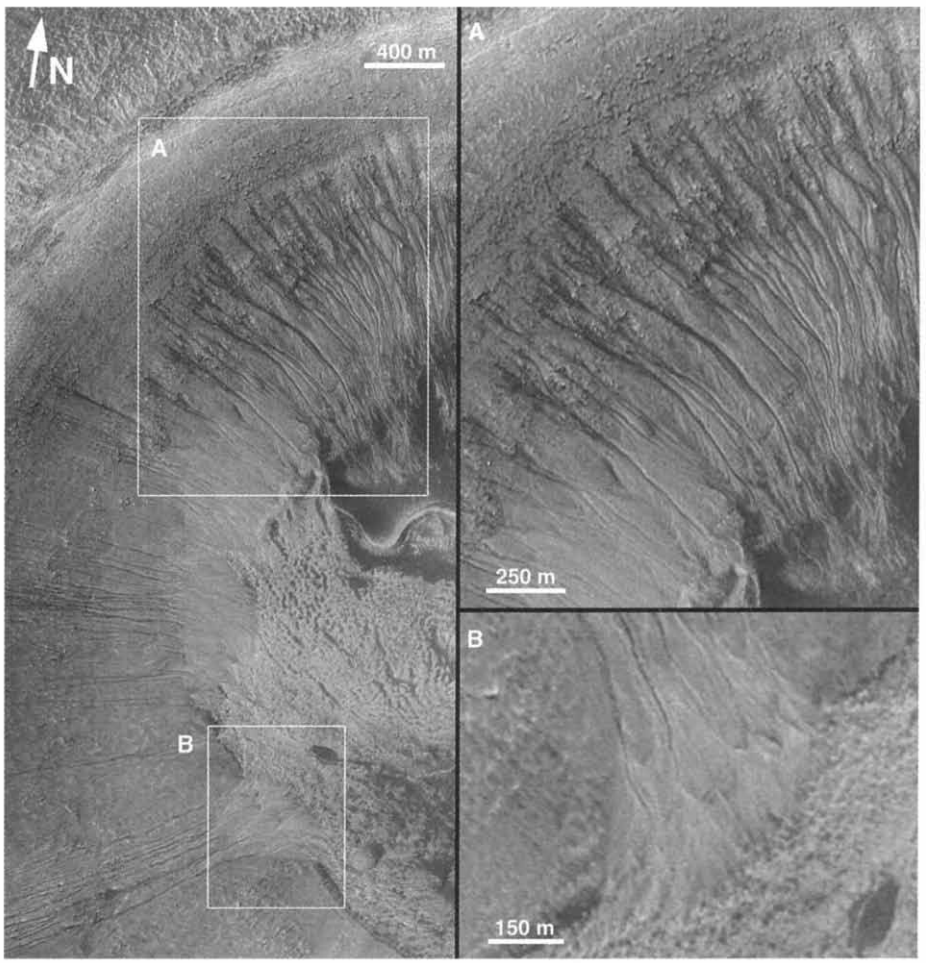

Fig. 5. In addition to contributory upper reaches, channels on aprons display distributary networks. Image and insets (**A** and **B**) are illuminated from the left and are subframes of MOC image M11-00944, located in a crater at 41.1°S, 159.8°W.

(Fig. 9C). These relations provide evidence that the seepage landforms are quite young, because superposed surfaces also lack impact craters and the superposed landforms are either ephemeral and/or dynamic (*31*).

Discussion

The martian landforms resemble terrestrial gullies, which form by a combination of processes, including overland flow, headward sapping (*32*), debris flow, and other mass movements (*33*)—all processes that, on Earth, involve the action of water. Stimulated by the problems raised by maintaining water as a liquid in the environments in which these features occur on Mars (*34*), we have sought evidence of other origins. However, it is unlikely that "dry" mass movement processes (such as granular flows or avalanches fluidized by atmospheric or soil gases) can explain the observed landforms. There are many instances of mass movements on slopes on Mars—indeed, every crater and depression on Mars seen by the MOC or earlier spacecraft exhibit such landforms—but the martian "gullies" described here are rare and easily differentiated from most of the other martian slope landforms. In many cases, the more common forms of mass movements are found on equator-facing slopes of craters that have alcove, channel, and apron landforms on their pole-facing slopes. These other landforms share many characteristics with landforms on the moon and Earth related to dry mass movements, reinforcing the impression that these gullies are different.

Other attributes of these landforms provide evidence for fluid erosion. Head alcoves are often associated with distinct layers within a cliff (e.g., Fig. 3, A and E); where they occur in groups on a wall with a single prominent layer, all the alcoves head within this layer. The distal, tapered portion of the alcoves (and the head of the main channel) occurs at the base of the bed, suggesting that this point is the location where undermining and collapse are initiated and from which material has been transported downslope in a manner that facilitates entrenchment. The main and secondary channels display characteristics of fluid flow, including sinuous paths, branched and/or anastomotic reaches, levees, streamlining, super-elevated banking, and incision. Many aprons show patterns in morphology that mimic those seen on terrestrial alluvial fans, including a filigree of distally diverging medial to marginal lineations (suggesting flow lines) and channels, lobate margins, and distal thinning. Another observation of note is that the channel heads and interiors, where visible, do not appear to be choked or clogged with debris, implying efficient transport throughout the conduit. The correlation between latitude and occurrence of these landforms, and their preponderance on poleward slopes, also suggests that there is a relation between the existence of these landforms and the presence of a volatile, such as water, that responds to solar insolation.

Despite the remote possibility that some unknown fluid might be responsible for these gullies, their attributes are most consistent with the action of water. The absence of geographic association of these features with volcanic terrains (Fig. 1) or obvious thermal sources (*35*), although at the same time showing latitudinal and azimuthal orientation relations, suggests that surficial environmental factors and not geothermal processes control their development.

Alcoves that are high on the walls of craters (but below the level of the preimpact surface), or high on the walls of grabens or other depressions, suggest that the water involved in creating these gullies must occur at shallow depths beneath the martian surface. Examination of available Mars Orbiter Laser Altimeter data shows that the seepage locations are only a few hundred meters or less below the surface.

The volume of water involved in the formation of the gullies is unknown. Conservative speculative scaling calculations (*36*) suggest that the formation of each apron may have involved a few thousand cubic meters of water. In some locations, the number of gullies and the area covered by their aprons suggest that the abundance of water might have been greater by a factor of 100 or more. Clusters of sites with limited spatial extent (as seen in grabens near Gorgonum Chaos, within Newton crater, in the pitted plains of the south polar region, and along Nirgal Vallis and Dao Vallis) argue for restricted source regions (reservoirs or aquifers).

A simplistic model of the processes by which these gullies form would involve groundwater moving within and along bedrock layers until it was exposed at the surface within depressions whose walls truncate the beds. Undermining and collapse of a region above the site of seepage would promote headward extension of an alcove, and surface runoff (and perhaps piping within colluvia)

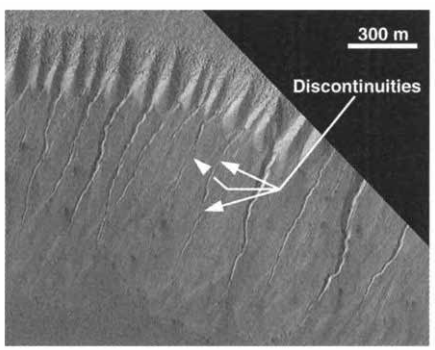

Fig. 6. Discontinuous reaches of some gullies (arrows) suggest that subsurface flow (or piping) may contribute to gully development. Illuminated from the upper left, this is a subframe of MOC image M03-02709, located at 70.8°S, 355.8°W.

Fig. 7. Contributory anastomosing pattern in portions of some gullies suggests the confluence of several streams of flow from the alcove into the main channel. Illuminated from the upper left, this is a subframe of MOC image M07-03298, near 46.9°S, 51.0°W.

Fig. 8. Example of an apron with digitate flows. Illuminated from the left, this is a subframe of MOC image M04-02479, near 40.0°S, 251.8°W.

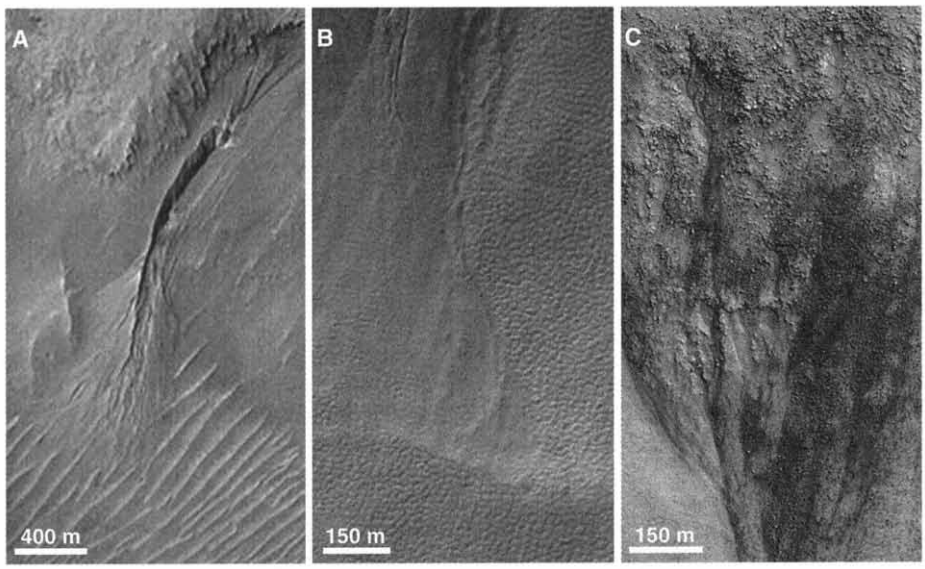

Fig. 9. Age relations between gullies and other landforms. (**A**) The best example of an apron that partly covers and obscures eolian bedforms in Nirgal Vallis. Illuminated from the upper left, this is a subframe of MOC image M07-00752, near 29.4°S, 39.1°W; north is toward the upper right. (**B**) Superposition of apron material on polygonal-patterned ground. Illuminated from the upper left, this is a subframe of MOC image M03-00537; north is toward the upper right. (**C**) Unmantled, bouldery, and mottled surface of a large alcove in the upper western wall of a crater at 65°S, 15°W. Illuminated from the upper right, this is a subframe of MOC image M11-00530; north is toward the lower right.

would remove debris accumulating at the seepage site. The resulting landform combines elements of a "classic" landslide promoted by groundwater and soil water with elements of surface runoff from a limited groundwater source. The location of the gullies (both in latitude and on nonequator-facing slopes) implies that the gradual percolation of groundwater to the surface and its evaporation as it emerges must be impeded, perhaps by an ice barrier that accumulates over time. In this model, a reservoir of liquid forms beneath this barrier, and the eventual, short-lived outburst from this ephemeral reservoir transports the accumulated debris downslope and out into the apron as a slurry flow of ice, liquid, and rock debris. The limited runout distance at the base of the slopes supports this idea. In this model, higher temperatures (closer to the equator and on equator-facing slopes) quickly evaporate emergent groundwater, preventing the persistence necessary to create gullies. Although the available evidence suggests that the processes that created these landforms acted in the relatively recent past and could even be contemporary, the absence of old, degraded, or cratered examples remains a mystery.

References and Notes

1. The debate over whether liquid water or some other liquid is responsible for fluid erosional landforms on Mars (including but not limited to the martian outflow channels and valley networks) is not specifically addressed in this work. Most geoscientists familiar with the martian landforms agree that water is the most likely candidate fluid (*2*); the only alternative is to speculate that some other completely unknown agent with properties essentially identical to those of water is or has been at work on Mars.
2. V. R. Baker *et al.*, *Geol. Soc. Am. Bull.* **94**, 1035 (1983).
3. D. J. Milton, *J. Geophys. Res.* **78**, 4037 (1973).
4. C. Sagan *et al.*, *Science* **181**, 1045 (1973).
5. V. R. Baker and D. J. Milton, *Icarus* **23**, 27 (1974).
6. R. P. Sharp and M. C. Malin, *Geol. Soc. Am. Bull.* **86**, 593 (1975).
7. D. C. Pieri, *Icarus* **27**, 25 (1976).
8. M. C. Malin, *J. Geophys. Res.* **81**, 4825 (1976).
9. H. Masursky *et al.*, *J. Geophys. Res.* **82**, 4016 (1977).
10. V. R. Baker and R. C. Kochel, *J. Geophys. Res.* **84**, 7961 (1979).
11. D. C. Pieri, *Science* **210**, 895 (1980).
12. A. V. Sidorenko, Ed., *The Surface of Mars* (Nauka, Moscow, 1980) (in Russian).
13. V. R. Baker, *The Channels of Mars* (Univ. of Texas Press, Austin, 1982).
14. M .H. Carr, *Water on Mars* (Oxford Univ. Press, New York, 1996).
15. P. H. Smith *et al.*, *Science* **278**, 1758 (1997).
16. A. W. Ward *et al.*, *J. Geophys. Res.* **104**, 8555 (1999).
17. M. P. Golombek *et al.*, *Science* **278**, 1743 (1997).
18. MGS reached Mars on 12 September 1997 and began >1 year of effort to achieve a circular polar-mapping orbit. The mapping phase of the mission began in March 1999 and is scheduled to conclude in January 2001. An extended mission phase might follow. For a description of the mission and its schedule, see (*37*) and (*38*).
19. M. C. Malin and M. H. Carr, *Nature* **397**, 589 (1999).
20. M. C. Malin and K. S. Edgett, *Lunar Planet. Sci.* **XXXI** (abstr. 1189) (2000) [CD-ROM].
21. M. H. Carr *et al.*, in preparation.
22. MOC images acquired during the Aerobraking 1 phase of the mission in late 1997 showed what we considered at the time to be possible evidence for seepage, including the walls of a crater at 65°S, 15°W (image AB1-07707), the walls and floor of a neighboring crater at 67°S, 15°W (image AB1-07708), and the walls of Nirgal Vallis (image AB1-00605). No images acquired in 1998 showed such landforms. Only when high-latitude southern hemisphere targets were again accessible to the MOC in 1999 were these features seen again.
23. The MOC high-resolution camera cannot acquire images continuously, because its data acquisition rate is more than a factor of 1000 higher than the rate at which the data can be recorded by the spacecraft for transmission to Earth. Images are limited by the 80-Mbit buffer within the camera. Observing a specific feature on Mars requires that an orbit passes over the feature and that manual inspection recognizes and designates an image to be taken of the potential target. Imaging attempts are based on semiweekly orbit position predictions with uncertainties typically larger than the camera's field of view, the targeting inspection of Viking orbiter images that are over 100 times lower in resolution than MOC pictures, and uncertainty in the actual spacecraft position in relation to surface features that exceeds 20 km in places. For a description of the MOC experiment, see (*39*).
24. C. F. S. Sharpe, *Landslides and Related Phenomena* (Cooper Square, New York, 1939).
25. D. J. Varnes, in *Landslides and Engineering Practice*, E. B. Eckel, Ed. (National Academy of Sciences, National Research Council, Highway Research Board, Washington, DC, 1958), pp. 20–47.
26. D. J. Varnes, in *Landslides, Analysis, and Control*, R. L. Shuster and R. J. Kriszek, Eds. (National Academy of Sciences, National Research Council, Transportation Research Board, Washington, DC, 1978), pp. 11–33.
27. C. G. Higgins, *Geology* **10**, 147 (1982).
28. A. D. Howard *et al.*, Eds., *NASA Spec. Publ. NASA SP-491* (1988).
29. V. R. Baker *et al.*, *Geol. Soc. Am. Spec. Pap. 252* (1990), pp. 235–265.
30. The ages of features on other planets are typically difficult to establish, because the only indications of age are geomorphic and hence subject to large uncertainty. The traditional ways of telling relative age—superposition of one feature on top of another and crosscutting of one feature by another—have been adapted to extraterrestrial surfaces. On Mars, as on other planets with solid surfaces, the abundance of impact craters is often taken as a proxy for determination of age: The more craters superposed on a surface, the older the surface. Unfortunately, it is much more difficult to establish the age of a surface devoid of craters because of the uncertainties associated with the stochastic nature of impact bombardment.
31. The time scales over which processes create or modify eolian bedforms and patterned ground are typically very short. Although comparisons of MOC and Viking images have not shown any bedforms to have moved in the past 20 years (at the scale of tens of meters) (*40, 41*), their forms and locations suggest that they have been active relatively recently in martian history (*40*). On Earth, polygonally patterned ground typically forms in periglacial environments by repeated thermal cycling at and below the melting temperature of water [e.g., (*42–44*)]. Although a variety of formation mechanisms have been proposed, in all cases terrestrial patterned ground is thought to develop quite quickly on a geologic time scale; that is, polygons only take thousands to tens of thousands of years to form. Polygons can survive only for time scales of hundreds of thousands of years, even in areas where they are relics from past periods, owing to the fragility of the conditions under which they are developed and preserved. Thus, the martian landforms are probably older than 20 years but may be younger than a million years.
32. "Sapping" is a generic term applied to a host of processes that loosen and transport granular material away from an escarpment and that promote the further undermining and collapse of that escarpment (*27–29*). It is a process that typically proceeds headward; that is, it starts at the outflow point of a source of fluid and migrates toward the fluid source. In the case of springs, sapping occurs at the seepage line. From that point, alluvial and colluvial processes create deposits downslope, and sapping undermines and promotes collapse above the seepage line, creating alcoves. A closely related terrestrial process is "piping," which involves the percolation or flow of subsurface fluid with sufficient pressure (flow or pore) to entrain materials (*45–47*). This entrainment removes support for overlying material, first creating irregular pits but often eventually leading to curvilinear depressions that resemble, or

become through other processes, conduits for surficial runoff. On Earth, both sapping and piping occur together with other processes that operate to remove their debris products. Without such removal, the groundwater processes choke in their own detritus. In terrestrial desert settings, flash floods are essential to removing the accumulated products (*48*). Where the eroding bedrock is sandstone, wind transport also plays an important role in removing debris.

33. C. G. Higgins *et al.*, *Geol. Soc. Am. Spec. Pap. 252* (1990), pp. 139–155.
34. It is difficult to reconcile the environments where the gullies are observed with an origin requiring liquid water because of the cold temperatures and low atmospheric pressures. Being polar and subpolar, these features spend as much as half a martian year at or near the freezing point of carbon dioxide (at martian pressures, ~148 K), or nearly 125 K below the triple point of water. Further, they occur on predominantly poleward-facing slopes, which are subject to substantially lower solar insolation and hence lower temperatures at any given latitude than the insolation and temperatures of adjacent flat, east/west, or equator-facing slopes. Most gullies occur in the southern hemisphere, which has a relatively high elevation, and hence at lower atmospheric pressure (increasing the evaporation rate).
35. The only exceptions are the gullies in the south- and southeast-facing walls of Dao Vallis, which heads within and follows a course though materials associated with the ancient highland volcano, Hadriaca Patera.
36. An estimate of the minimum amount of water that may have participated in the formation of the gullies can be made as follows. We assume that the aprons were formed primarily by debris flows. Field and laboratory measurements [e.g., (*49*, *50*)] indicate that such flows contain no less than 10% by volume water and typically no more than 30% by volume (little or no mobility occurs with lower water content; higher water content leads to mudflows or hyperconcentrated stream flow). Aprons vary substantially in area; those seen in Fig. 5 cover ~1.25 million square meters. Assuming a thickness of ~2 m and a volume fraction of 10% leads to a water volume of 250,000 m^3 (250 million liters or 66 million gallons). For reference, if fully accessible, this would be enough water to supply 100 people for nearly 20 years (without recycling). About 100 channels feed these aprons, suggesting that each apron-forming event involves 2500 m^3 (2.5 million liters or 660,000 gallons) of water, enough for 20 people for a year. Factors that would reduce the amount of water include evaporation and/or sublimation of the water after emplacement; factors that may increase the amount include greater apron thickness and higher water volume fractions.
37. A. Albee, *Eos* **77** (no. 45), 441 (1996).
38. A. L. Albee *et al.*, *Science* **279**, 1671 (1998).
39. M. C. Malin *et al.*, *J. Geophys. Res.* **97**, 7699 (1992).
40. K. S. Edgett and M. C. Malin, *J. Geophys. Res.* **105**, 1623 (2000).
41. J. R. Zimbelman, *Geophys. Res. Lett.* **27**, 1069 (2000).
42. A. L. Washburn, *Geol. Soc. Am. Bull.* **67**, 823 (1956).
43. R. F. Black, *Quat. Res.* **6**, 3 (1976).
44. A. H. Lachenbruch, *Geol. Soc. Am. Spec. Pap. 70* (1962).
45. C. G. Higgins, in *Groundwater as a Geomorphic Agent*, R. G. LaFleur, Ed. (Allen & Unwin, Boston, 1984), pp. 18–58.
46. G. G. Parker Sr. *et al.*, *Geol. Soc. Am. Spec. Pap. 252* (1990), pp. 77–110.
47. R. B. Bryan and J. A. A. Jones, *Geomorphology* **20**, 209 (1997).
48. J. E. Laity and M. C. Malin, *Geol. Soc. Am. Bull.* **96**, 203 (1985).
49. J. Fink *et al.*, *Geophys. Res. Lett.* **8**, 43 (1981).
50. C. J. Kafura, thesis, Arizona State University, Tempe (1988).
51. The authors express their appreciation to M. Caplinger, E. Jensen, S. Davis, W. Gross, D. Michna, J. Sandoval, K. Supulver, and J. Warren for their efforts in support of the MOC. Without their hard work and dedication, the images on which this work is based would not have been acquired. W. Dietrich provided early guidance to consideration of the origin of the landforms described here. Comments by two anonymous referees provided useful perspectives on our results. This work was supported by Jet Propulsion Laboratory contracts 959060 and 1200780.

3 April 2000; accepted 16 May 2000

REPORTS

Microrobots for Micrometer-Size Objects in Aqueous Media: Potential Tools for Single-Cell Manipulation

Edwin W. H. Jager,* Olle Inganäs, Ingemar Lundström

Conducting polymers are excellent materials for actuators that are operated in aqueous media. Microactuators based on polypyrrole-gold bilayers enable large movement of structures attached to these actuators and are of particular interest for the manipulation of biological objects, such as single cells. A fabrication method for creating individually addressable and controllable polypyrrole-gold microactuators was developed. With these individually controlled microactuators, a micrometer-size manipulator, or microrobotic arm, was fabricated. This microrobotic arm can pick up, lift, move, and place micrometer-size objects within an area of about 250 micrometers by 100 micrometers, making the microrobot an excellent tool for single-cell manipulation.

The development of tools for the manipulation of single cells is of major importance for the rapidly growing area of genomics and proteomics, particularly in massively parallel single-cell manipulation and characterization. Actuators for the positioning and moving of objects such as cells must be compatible with the living conditions for cells. Optical tweezers fulfill some of these criteria, but they are not suited to massively parallel characterization; field cages (*1*) offer both possibilities. Here, we demonstrate an alternative in the form of a microrobotic arm operating in an aqueous environment, with dimensions suitable and scalable for the manipulation of cells. Our microfabricated devices are built on conjugated polymers used as the active element of a bending bilayer, which generates large-amplitude motion. Patterning of active and passive elements defines the geometry of a microrobot, whose individual bending beams are addressed separately and are therefore capable of more complex motions. We demonstrate the gripping and positioning of 100-μm objects with this microrobotic arm.

The term "microrobot" is often used for centimeter-size miniature robots built by conventional methods, combined with microelectronics for control. In our view, microrobots are millimeter and submillimeter devices with individual parts of micrometer size built by micromachining technology. Parts for such microrobots include hollow triangular robot links made of polycrystalline silicon (polysilicon) (*2*), in which systems of rods and levers are used to rotate the links out of plane of a substrate; wings for artificial flying insects based on polysilicon plates attached to polyimide hinges (*3*); and polysilicon microgrippers (*4*). An example of a complete microrobot is the walking silicon microrobot (*5*). The actuation here is based on the thermal expansion of polyimide deposited in V-shaped grooves etched in silicon with integrated heaters. However, none of these operate in water, and they would not be suitable as microactuators for the manipulation of cells.

Conducting polymers like polypyrrole (PPy) and polyaniline are excellent materials for actuators. Both macro- (*6–10*) and microactuators (*11–14*) based on these materials have been presented in the literature. These actuators are based on the reversible volume change of the conducting polymers upon oxidation and reduction. For the microactuators, we normally use PPy(DBS) (polypyrrole doped with dodecyl benzene sulfonate ions) in a bilayer configuration with Au acting as both a structural layer and an electrode. When we apply a negative potential on the Au (−1 V versus Ag/AgCl), we reduce the PPy to its neutral state [PPy^0 (Na^+DBS^-)]. To maintain charge neutrality,

Department of Physics and Measurement Technology, Division of Applied Physics, Linköpings universitet, S-581 83, Linköping, Sweden.

*To whom correspondence should be addressed. E-mail: edjag@ifm.liu.se